An analytical model for the detection of levitated nanoparticles in optomechanics

A. T. M. Anishur Rahman, A. C. Frangeskou, P. F. Barker, and G. W. Morley

Citation: Review of Scientific Instruments **89**, 023109 (2018); doi: 10.1063/1.5008396
View online: https://doi.org/10.1063/1.5008396
View Table of Contents: http://aip.scitation.org/toc/rsi/89/2
Published by the American Institute of Physics

An analytical model for the detection of levitated nanoparticles in optomechanics

A. T. M. Anishur Rahman,[1,2,a)] A. C. Frangeskou,[2] P. F. Barker,[1] and G. W. Morley[2]
[1]*Department of Physics and Astronomy, University College London, Gower Street, London WC1E 6BT, United Kingdom*
[2]*Department of Physics, University of Warwick, Gibbet Hill Road, Coventry CV4 7AL, United Kingdom*

(Received 5 October 2017; accepted 15 January 2018; published online 9 February 2018)

Interferometric position detection of levitated particles is crucial for the centre-of-mass (CM) motion cooling and manipulation of levitated particles. In combination with balanced detection and feedback cooling, this system has provided picometer scale position sensitivity, zeptonewton force detection, and sub-millikelvin CM temperatures. In this article, we develop an analytical model of this detection system and compare its performance with experimental results allowing us to explain the presence of spurious frequencies in the spectra. https://doi.org/10.1063/1.5008396

I. INTRODUCTION

In the past, interferometric position detection systems have been used in optomechanics for the detection of zeptonewton scale forces,[1–3] the demonstration of sub-kelvin centre-of-mass (CM) temperatures,[4–6] the measurement of Brownian motions,[7] and the manipulation of levitated particles.[8–12] Furthermore, this system has provided pm/$\sqrt{\text{Hz}}$ position sensitivity.[4] In these schemes, a reference beam and the scattered light from a levitated particle interfere on a photodiode. This interference produces a signal which is directly related to the instantaneous position of the oscillator. After Fourier transformation, oscillation frequencies (ω_x, ω_y, and ω_z) along the three axes can be retrieved from the position signals. Subsequently, these frequencies are used for parametric feedback cooling to actively control the motion of a levitated particle.[1–3,5,8–14] As with other interferometric schemes, this system is well known for its high precision and resilience to noise. In optomechanical setups, this is further enhanced by a balanced detection system. A balanced detector consists of two matched photodiodes which help us to reduce common mode noise and other unwanted signals. Here, we develop a model of this interferometric scheme and present experimental evidence to justify its validity. We find that the predictions of our model match closely with the experimental results. We also show that due to the configuration of the balanced detector, it detects frequency along the desired axis as well as frequencies from the remaining two axes and the frequencies resulting from the various linear combinations of ω_x, ω_y, and ω_z. Finally, we discuss the possible side effects of these spurious frequencies on the performance of parametric feedback cooling.

II. INTERFEROMETRIC DETECTION SCHEME

Figure 1 shows a schematic of a tweezer-based optomechanical experiment in which a high numerical aperture microscope objective forms the trap by tightly focusing a laser beam into a diffraction limited spot. The trap is normally placed inside a vacuum chamber. Once a desired particle is trapped, the chamber is evacuated and the position of the particle is monitored using the interferometric detection system. Let us assume that $\mathbf{r} = x\hat{x} + y\hat{y} + z\hat{z}$ is the instantaneous position vector of the levitated particle from the centre of the trap, where $x = A_x \sin(\omega_x t + \phi_x)$, $y = A_y \sin(\omega_y t + \phi_y)$, and $z = A_z \sin(\omega_z t + \phi_z)$ are the instantaneous distances of the particle along the x, y, and z axes. The angular trap frequencies are ω_x, ω_y, and ω_z, and A_x, A_y, and A_z are the respective amplitudes of oscillations along the three axes. Likewise, ϕ_x, ϕ_y, and ϕ_z are the phases along the three axes. In order to detect and manipulate the position of the levitated particle, balanced photo-detectors are placed along the various axes. As an example, in Fig. 1, we show one detector placed along the x-axis. This enables us to detect the trap frequency along the x-axis. From the geometry of the problem, the position vectors of the two photodiodes (D_1 and D_2 in Fig. 1) from the centre of the trap are $\mathbf{r_1^0} = x_0\hat{x} + y_0\hat{y} + z_0\hat{z}$ and $\mathbf{r_2^0} = -(x_0 + \Delta x)\hat{x} + y_0\hat{y} + z_0\hat{z}$, where x_0, y_0, and z_0 are the distances of the two photodiodes from the centre of the trap. Δx is the position mismatch between the two photodiodes along the x-axis. This mismatch initiates an imbalance in the detector (see below for details). The distances of a levitated particle from the two photodiodes of the balanced detector can be written as $r_1 = |-\mathbf{r} + \mathbf{r_1^0}| = \sqrt{r_0^2 + r^2 - 2x_0x - 2y_0y - 2z_0z}$ and $r_2 = |-\mathbf{r} + \mathbf{r_2^0}| = \sqrt{r_0^2 + r^2 + 2x_0x - 2y_0y - 2z_0z + \Delta x(\Delta x + 2x + 2x_0)}$, where $r_0 = \sqrt{x_0^2 + y_0^2 + z_0^2}$.

Let us also assume that at the focus of the trap the y–polarized electric field can be expressed[15,16] as $\mathbf{E}_l = \frac{E_0 w_0}{w(z)} \exp\left[-\frac{x^2+y^2}{w(z)^2}\right] \exp\left[i\omega t - ikz - i\frac{k(x^2+y^2)}{2R(z)} + i\zeta(z)\right]\hat{y}$, where $k = 2\pi/\lambda$, $\omega = 2\pi c/\lambda$, and λ and c are the trapping laser wavelength and speed in free space, respectively. $w(z) = w_0\sqrt{1 + z^2/z_r^2}$, $R(z) = z(1 + z_r^2/z^2)$, $\zeta = \tan^{-1} z/z_r$, and $w_0 = \sqrt{\lambda z_r/\pi}$, where z_r is the Rayleigh range. E_0 can be expressed as $\sqrt{2I_0/\epsilon_0 c}$,

a)Electronic mail: a.rahman@ucl.ac.uk

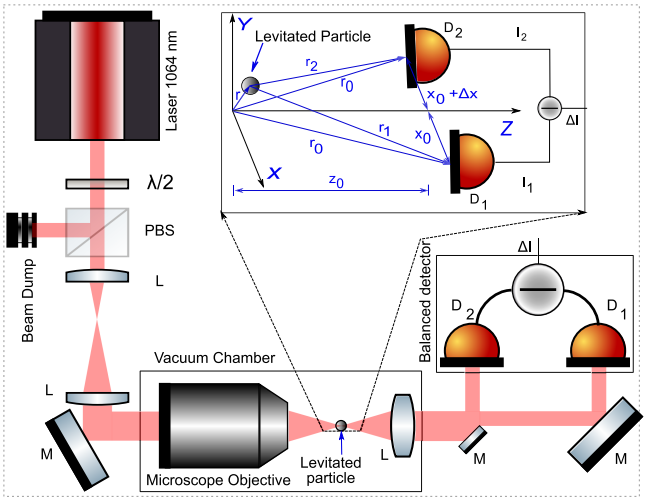

FIG. 1. A schematic of our tweezer-based optomechanical system along with the interferometric detection system along the x-axis. The origin of the coordinate system is the centre of the trap. The inset shows the levitated particle along with the detection system in the co-ordinate system. Note that z_0 actually signifies the distance between the levitated particle and the lens after it. Since the light is collimated after the lens, the distance between the lens and the diodes, shown for the sake of visualization in the main schematic, is not important. Further, different symbols correspond to L—lens, M—mirror, PBS—polarizing beam splitter, $\lambda/2$—halfwave plate, and D—diodes.

where I_0 is the intensity of a Gaussian trapping laser beam at the focus and ϵ_0 is the dielectric constant of free space. The electric field induces a dipole moment in the trapped particle. This leads to a surface charge density if the polarization is uniform throughout the trapped bead or a volume charge density otherwise.[17]

Once a charge is induced inside a particle, it starts to oscillate in the oscillating trapping field, and an oscillating charge radiates/scatters light. The scattered field from a Rayleigh spherical particle ($a << \lambda$) that a photodiode receives can be expressed as[18]

$$\begin{aligned}\mathbf{E_{s_1}} \approx & -\frac{Ak^2}{4\pi r_1^3}\left(x_0^2+z_0^2+x^2+z^2-2x_0x-2z_0z\right)\\ & \times E_0\exp\{i\,(\omega t-kz_0\,(1+\frac{x_0^2+y_0^2}{2z_0^2}\\ & +\frac{r^2-2x_0x-2y_0y-2z_0z}{2z_0^2}))\}\hat{y},\end{aligned}\tag{1}$$

$$\begin{aligned}\mathbf{E_{s_2}} \approx & -\frac{Ak^2}{4\pi r_2^3}\left(x_0^2+z_0^2+x^2+z^2+2x_0x+2\Delta xx_0-2z_0z\right)\\ & \times E_0\exp\{i\,(\omega t-kz_0\,(1+\frac{x_0^2+y_0^2}{2z_0^2}\\ & +\frac{r^2+2x_0x-2y_0y-2z_0z}{2z_0^2}+\frac{\Delta xx_0}{z_0^2}))\}\hat{y},\end{aligned}$$

where $A = 4\pi a^3\epsilon_0(\epsilon-1)/(\epsilon+2)$, ϵ, and a are the polarizablity, dielectric constant, and radius of the levitated particle, respectively. We have also assumed that the electric field (E_0) remains constant over the distance a levitated particle traverses inside the trap. This is valid when the amplitude of oscillation of a levitated particle is small compared to the beam waist $w_0 = \lambda/(\pi NA)$, where NA is the numerical aperture of the trapping lens and λ is the trapping laser wavelength.

In addition to the scattered light from the levitated particle, each photodiode also receives directly transmitted laser light from the trapping beam. In the far-field where $z_0 >> z_r$ and $(x_0^2+y_0^2) << z_0^2$, the directly transmitted beam unperturbed by the levitated particle can be expressed as[15] [see Eqs. (A1) and (A2) of the Appendix]

$$\begin{aligned}\mathbf{E_{T_1}} &\approx \frac{z_rE_0}{z_0}\exp\left[i\omega t-ikz_0(1+\frac{x_0^2+y_0^2}{2z_0^2})+\pi/2\right]\hat{y},\\ \mathbf{E_{T_2}} &\approx \frac{z_rE_0}{z_0}\exp\left[i\omega t-ikz_0(1+\frac{x_0^2+y_0^2}{2z_0^2})+\pi/2\right]\\ &\quad\times\exp(-i\frac{\Delta xx_0k}{z_0})\hat{y},\end{aligned}\tag{2}$$

where $\pi/2$ is the Gouy phase shift.

Considering the scattered field, and the field due to the directly transmitted light together, the difference in intensity $\Delta I = I_{D_2} - I_{D_1}$ that a balanced detector produces [see Eqs. (A6)–(A9) of the Appendix for derivations] can be written as

$$\begin{aligned}\Delta I \approx & \overbrace{\frac{x_0xA^2k^4}{2\pi^2z_0^6}\left(x_0^2+z_0^2+x^2+z^2-2z_0z\right)I_0}^{Scattering}-\overbrace{\frac{Ak^2}{\pi z_0^3}\left(x_0^2+z_0^2+x^2+z^2-2z_0z\right)\cos\left(k\frac{r^2-2y_0y-2z_0z}{2z_0}\right)\sin\left(\frac{x_0xk}{z_0}\right)\frac{z_r}{z_0}I_0}^{Interference}\\ & -\overbrace{\frac{2x_0xAk^2}{\pi z_0^3}\sin\left(k\frac{r^2-2y_0y-2z_0z}{2z_0}\right)\cos\left(\frac{x_0xk}{z_0}\right)\frac{z_r\epsilon_0cE_0^2}{2z_0}}^{Interference}\\ & -\overbrace{\frac{\Delta xx_0Ak^3}{2\pi z_0^4}\left(x_0^2+z_0^2+x^2+z^2-2z_0z+2x_0x\right)\cos\left(k(\frac{r^2-2y_0y-2z_0z}{2z_0}+\frac{x_0x}{z_0})\right)\frac{z_r}{z_0}I_0}^{Imbalance},\end{aligned}\tag{3}$$

where we have assumed $I_0 = \epsilon_0 c E_0^2/2$, $\alpha = \Delta x x_0 k/z_0$, ($x_0$, y_0, x, y, z) << z_0, $1/r_1 \approx 1/z_0$, and $1/r_2 \approx 1/z_0$. Further, we have assumed that the depolarization of the scattered light is negligible. This is true when the levitated particle is small ($a << \lambda$) compared to the trapping laser's wavelength. It can be seen that there are three main terms in the signal that a balanced detector produces. These are an interference term consisting of the scattered and unscattered light, a term due to the scattered light alone, and a term owing to the imbalance ($\alpha > 0$) between the two arms of a balanced detector. In the ideal scenario, where the two arms of a balanced photodetector are perfectly balanced $\Delta I_{Imb} = 0$ ($\alpha = 0$). Further, the contribution of the scattering term in the overall signal is much smaller than the interference term. As a result, below we only analyze the interference term and the term due to the imbalance and show their importance in the context of balanced detection.

Expanding $\cos\left(k\frac{r^2-2y_0y-2z_0z}{2z_0}\right)$, $\sin\left(k\frac{r^2-2y_0y-2z_0z}{2z_0}\right)$, $\cos\left(\frac{x_0xk}{z_0}\right)$, and $\sin\left(\frac{x_0xk}{z_0}\right)$ into their respective Taylor series and keeping only lower order terms, and substituting $x = A_x \sin\omega_x t$, $y = A_y \sin\omega_y t$, and $z = A_z \sin\omega_z t$, the interference term can be written as [see Eq. (A10) of the Appendix for details]

$$\Delta I_{Inter} = -\frac{x_0 z_r A k^3}{\pi z_0^5} I_0 \left[(x_0^2 + z_0^2)A_x \sin\omega_x t - 2z_0 A_x A_z \times \cos(\omega_x - \omega_z)t + 2z_0 A_x A_z \cos(\omega_x + \omega_z)t + \mathrm{f}(\omega_\mathrm{x}, \omega_\mathrm{y}, \omega_\mathrm{z})\right] I_0, \quad (4)$$

where we have assumed $\phi_x = \phi_y = \phi_z = 0$ for simplicity.

From Eq. (4), one can find that even though the balanced detector in the configuration shown in Fig. 1 is meant to detect the oscillation frequency along the x-axis, our model predicts the detection of many other frequencies f(ω_x, ω_y, ω_z) in addition to ω_x. To justify the validity of Eq. (4), Fig. 2(b) shows a Fourier transform of the measured time domain signal obtained using a balanced photodiode (PDB210C/M—Large-area balanced photodetector, Thorlabs, Ltd.) from our levitated experiment. In this particular case, a 50 nm silica particle was levitated using a dipole trap and data were collected at 3 mbar. Immediately, one can recognize the desired frequency along the x-axis, $\omega_x/2\pi$. One can also find two shoulders at $\omega_x - \omega_z$ and $\omega_x + \omega_z$ as predicted in Eq. (4). These frequencies are much weaker than ω_x as understandable from Eq. (4). Elaborately, from our experiment, we have $A_x \approx A_y \approx A_z/2 \approx 100$ nm, $x_0 = y_0 = 1$ mm, and $r_0 \approx z_0 = 10$ mm. On substitution of these values in Eq. (4), one finds the ratio of the amplitudes of $\omega_x - \omega_z$ or $\omega_x + \omega_z$, and ω_x is $2A_z/z_0 \approx 4 \times 10^{-5}$, which is small and only in qualitative agreement with our experimental data [see Fig. 2(b)]. Mismatch between the ratios of the amplitudes of the experimental data and the theoretical model can be attributed to the different approximations and assumptions we have made in deriving the theoretical model. Other frequencies as appeared in Eq. (4) are about two orders of magnitude weaker than $\omega_x - \omega_z$ or $\omega_x + \omega_z$. This is good for parametric feedback cooling where frequencies other than the desired frequency are problematic. A consequence of the unwanted frequencies is that they impart amplitude modulation to the intensity of the desired signal as can be seen in Fig. 2(a). This has been observed in earlier experiments[1,5] as well.

The appearance of ω_z and its harmonics in Fig. 2 are not expected according to Eq. (4). Nevertheless, it can be explained by analyzing the impact of the imbalance between the two arms of a balanced detector. Specifically, in theory, $\alpha = 0$ is achievable, but in a realistic laboratory environment, a minor imbalance between the two detectors is unavoidable. The consequence of this unwanted imbalance can be quite significant. For example, the ratio between the dominant imbalance [ω_z, see Eq. (A11) of the Appendix] and interference [ω_x, 1st term in Eq. (4)] terms is $\approx 2\Delta x/z_0$. If one considers $\Delta x = 0.01 z_0$, then the ratio of these two terms is ≈ 0.02. This is equivalent to 2% of the intensity along the x-axis and is non-trivial.

For larger particles, spurious frequencies become even more pronounced as we show in Fig. 3. In this example, data were collected using a 380 nm silica particle and the detector was set to detect the frequency along the x-axis. One can see that the intensities of ω_z and its harmonics as well as other frequencies are comparable to the intensity of ω_x. From our laboratory experience, this happens with the majority of the larger nanoparticles that we levitate using our dipole trap. A similar phenomenon has also been detected by other groups.[4] We believe that for the larger particles it is relatively easy to move outside the linear region of the trap to the non-linear part. This introduces coupling between the different modes of oscillations[8,9] and hence the appearances of frequencies other than the desired one. It is also plausible that strong scattering from large particles and the ensuing interference around the trapping region alters the trapping potential profile which introduces coupling between different axes that is otherwise assumed decoupled. We also believe that larger

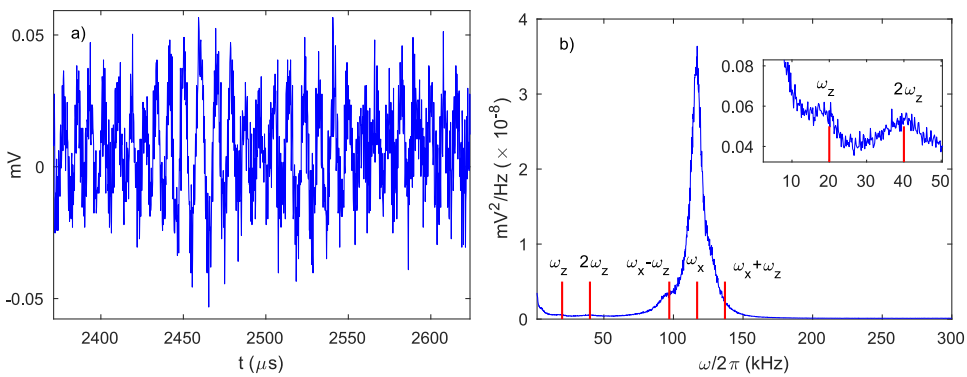

FIG. 2. A levitated silica nanoparticle (50 nm) at 3 mbars of pressure—(a) time trace as it oscillates inside the trap and (b) power spectral density. Red vertical lines in (b) represent some of the frequencies (except ω_z and its harmonics) predicted by Eq. (4). Data were collected at 3 mbars of pressure.

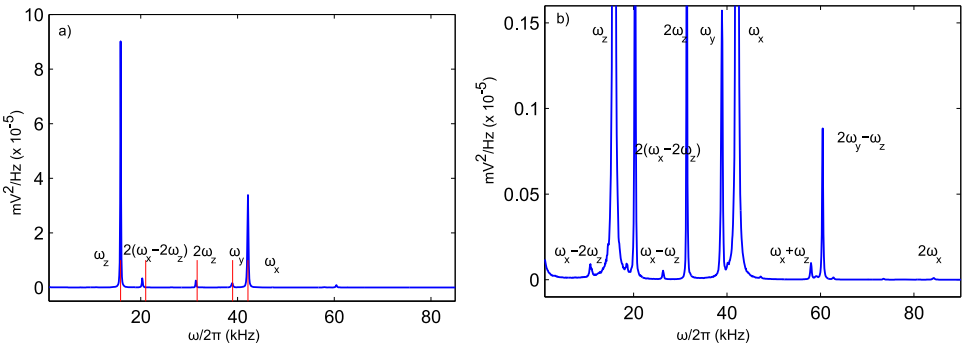

FIG. 3. Power spectral density (PSD) of a relatively large (380 nm) silica nanoparticle at 0.50 mbar in a dipole trap—(a) shows most of the dominant frequencies visible in the PSD while (b) is the zoomed view of (a).

particles modify the propagation path of the trapping light due to refraction more strongly than their smaller counterparts. This creates severe dynamic imbalance between the two arms of a detector as the particles oscillate inside the trap and leads to the appearance of unwanted frequencies. Further, as the trapped particle becomes large, the scattered light from the particle gets depolarized.[18] As a result, the interference between the scattered and the trapping light diminishes. Further, the assumption that the electric field remains constant over the distance the particle traverses breaks down.

In the extreme case of imbalance where $\alpha >> 0$, the balanced detector shown in Fig. 1 turns into an oscillation detector along the z-axis. Specifically, in the balanced detection of frequency along the z-axis, one arm of the balanced detector is fed with a fixed laser light which does not go through the trap, while the other arm of the detector is illuminated with the scattered plus the directly transmitted light that goes through the trap.[5] The role of the constant laser power in the first arm is to cancel the dc term that arises in the second photodiode. The overall model is shown in the following equation [see Eq. (A12) of the Appendix for derivation]:

$$\Delta I_z \approx \frac{z_r(x_0^2+z_0^2)k^3A}{4\pi z_0^5}\,(A_x^2\,\sin^2\,\omega_x t + A_y^2\,\sin^2\,\omega_y t + A_z^2\,\sin^2\,\omega_z t - 2x_0A_x\,\sin\,\omega_x t - 2y_0A_y\,\sin\,\omega_y t - 2z_0A_z\,\sin\,\omega_z t)\,I_0. \quad (5)$$

One can see that the detector for the z-axis detects the frequency along the desired axis as well as frequencies along the remaining two axes. Our model of the detector also predicts the detection of harmonics of the fundamental modes albeit very weakly. Experimental data from the z-axis detector in our levitated setup are shown in Fig. 4. In agreement with the model, in our experiment, we detect all three frequencies along the three laboratory axes. Our model also agrees with the experimental power spectral density data presented by Li *et al.* in Ref. 4 where frequencies along all three axes are visible.

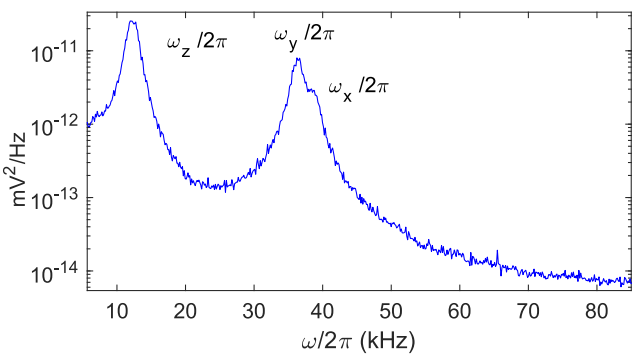

FIG. 4. Power spectral density from a balanced detector along the z-axis.

Finally, it is instructive to consider the impact of the unwanted frequencies in parametric feedback cooling—particularly in experiments where large particles are levitated. It is well known that as the particle size increases the separation in frequency among the different oscillation axes diminishes. These waning gaps in frequency require a proportional reduction in the bandwidths (BWs) of the filters used in parametric feedback cooling. At some point, a further reduction of the BW becomes un-viable and filters become ineffective in suppressing unwanted frequencies. Observing this phenomenon in our levitated experiments, we wanted to derive an analytical formulation that can predict the achievable CM temperature under certain frequency noises. However, we find that an analytical model of this situation can only be derived if the spurious frequencies are the harmonics of the fundamental modes (ω_x, ω_y, and ω_z) that one wants to cool. But this is not the case for these experiments. As a result, we are unable to provide an analytical solution of this situation. Nevertheless, we believe that an electrodynamic numerical simulation, which is not considered here, can provide quantitative answers of the impact of the unwanted frequencies in parametric feedback cooling.

III. CONCLUSIONS

We have developed a model which represents the combined interferometric and balanced detection schemes used in levitated optomechanics. According to our model, frequencies such as ω_x and its harmonics as well as the sum and differences of ω_x with the frequencies of oscillation along the remaining two axes and their harmonics are naturally expected from a balanced detector along the x-axis. However, the appearances of ω_y and ω_z and their harmonics in the detector along the x-axis can be attributed to the imbalance present in the detection system. An effect of these unwanted frequencies is the reduction of the signal to noise ratio, which might limit the ultimate temperature achievable in parametric feedback cooling. This is particularly true for systems involving large levitated particles. According to our model, designing the experiment to make x_0k/z_0 smaller will tend to reduce problems with imbalance as

$\alpha = \Delta x x_0 k/z_0$. In particular, making k smaller by using a longer wavelength laser for trapping seems appropriate. Reducing x_0 would also help but will reduce the amount of light that a detector receives.

ACKNOWLEDGMENTS

This work was supported by the United Kingdom EPSRC (Nos. EP/M013243/1 and EP/J014664/1). G.W.M. is supported by the Royal Society. Raw data is available at http://wrap.warwick.ac.uk/98256.

APPENDIX: DERIVATIONS

Exploiting the impulse response of free space propagation,[15] the directly transmitted light received by the photodiodes can be expressed as

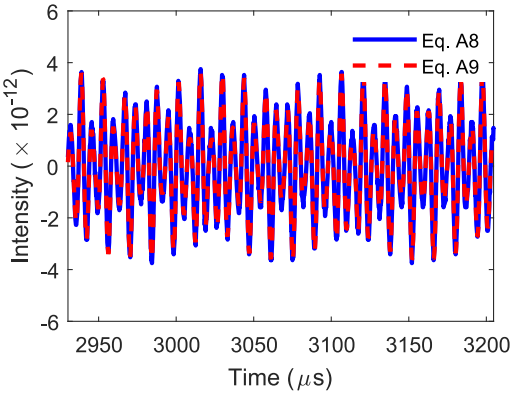

FIG. 5. Comparison between the exact difference signal Eq. (A8) (blue solid line) and approximate ΔI [Eq. (A9), red broken line] assuming $\alpha = 0$, $I_0 = 2.5 \times 10^{11}$ W/m^2, $x_0 = y_0 = 1$ mm, $z_0 = 10$ mm, $A_x = A_y = 100$ nm, $A_z = 200$ nm, $\omega_x = 143$ kHz, $\omega_y = 130$ kHz, $\omega_z = 33$ kHz, and $\phi_x = \phi_y = \phi_z = 0$.

$$
\begin{aligned}
E_{T_1}(x_0, y_0, z_0) &= \frac{i \exp[i\omega t - ikz_0]}{\lambda z_0} \int_\infty^\infty \int_\infty^\infty E_0 \exp[-\frac{x^2+y^2}{w_0^2}] \exp[-i\pi \frac{(x_0-x)^2+(y_0-y)^2}{\lambda z_0}] dxdy \\
&= \frac{iE_0 \exp[i\omega t - ikz_0]}{\lambda z_0} \exp[-i\pi \frac{x_0^2+y_0^2}{\lambda z_0}] \int_\infty^\infty \int_\infty^\infty \exp[-(\frac{1}{w_0^2} + \frac{i\pi}{\lambda z_0})x^2 + i\frac{2\pi x_0}{\lambda z_0} x] \\
&\quad \times \exp[-(\frac{1}{w_0^2} + \frac{i\pi}{\lambda z_0})y^2 + i\frac{2\pi y_0}{\lambda z_0} y] dxdy \\
&= \frac{iE_0 \exp[i\omega t - ikz_0]}{\lambda z_0} \exp[-i\pi \frac{x_0^2+y_0^2}{\lambda z_0}] \frac{\pi \lambda z_0 w_0^2}{\lambda z_0 + i\pi w_0^2} \exp[-\frac{\pi w_0^2 (x_0^2+y_0^2)}{\lambda z_0 (\lambda z_0 + i\pi w_0^2)}] \\
&= \frac{i\pi w_0^2}{\lambda z_0 + i\pi w_0^2} E_0 \exp[i\omega t - ikz_0] \exp[-i\pi \frac{x_0^2+y_0^2}{\lambda z_0}] \exp[-\frac{\pi w_0^2 (x_0^2+y_0^2)}{\lambda^2 z_0^2}] \\
&= \frac{E_0}{1 - i\frac{z_0}{z_r}} \exp\left[i\omega t - ikz_0 (1 + \frac{x_0^2+y_0^2}{2z_0^2})\right] \exp[-\frac{\pi w_0^2 (x_0^2+y_0^2)}{\lambda^2 z_0^2}] \\
&\approx \frac{E_0}{1 - i\frac{z_0}{z_r}} \exp\left[i\omega t - ikz_0 (1 + \frac{x_0^2+y_0^2}{2z_0^2})\right] \\
&\approx \frac{z_r E_0}{z_0} \exp\left[i\omega t - ikz_0 (1 + \frac{x_0^2+y_0^2}{2z_0^2}) + \arctan(\frac{z_0}{z_r})\right] \\
&\approx \frac{z_r E_0}{z_0} \exp\left[i\omega t - ikz_0 (1 + \frac{x_0^2+y_0^2}{2z_0^2}) + \pi/2\right], \\
\Re\{\mathbf{E_{T_1}}\} &= \frac{z_r}{z_0} E_0 \sin\left(\omega t - kz_0 (1 + \frac{x_0^2+y_0^2}{2z_0^2})\right) \hat{\mathbf{y}}, \qquad \text{(A1)}
\end{aligned}
$$

where we have used $\int_\infty^\infty \exp[-ax^2 + ibx] dx = \sqrt{\pi/a} \exp[-b^2/(4a)]$, $\frac{w_0^2}{\lambda r_0} << 1$, and $\exp[-\frac{\pi w_0^2 (x_0^2+y_0^2)}{\lambda^2 r_0^2}] \approx 1$. Similarly, E_{T_2} can be expressed as

$$
E_{T_2}(-x_0 - \Delta x, y_0, z_0) \approx \frac{z_r E_0}{z_0} \exp\left[i\omega t - ikz_0 (1 + \frac{x_0^2+y_0^2}{2z_0^2}) + \pi/2\right] \exp(-i\frac{\Delta x x_0 k}{z_0}). \qquad \text{(A2)}
$$

The scattered field received by the two photodiodes can be expressed as[18]

$$\begin{aligned}
\mathbf{E_{s_1}} &= \frac{Ak^2E_0}{4\pi r_1}\exp\{i(\omega t - kr_1)\}\Big[\frac{(x_0-x)(y_0-y)}{r_1^2}\hat{\mathbf{x}} - \frac{(x_0-x)^2+(z_0-z)^2}{r_1^2}\hat{\mathbf{y}} + \frac{(z_0-z)(y_0-y)}{r_1^2}\hat{\mathbf{z}}\Big] \\
&\approx -\frac{Ak^2\left[(x_0-x)^2+(z_0-z)^2\right]}{4\pi r_1^3}E_0\exp\{i(\omega t - kr_1)\}\hat{\mathbf{y}} \\
&= -\Big[\frac{A(x_0^2+z_0^2)k^2}{4\pi r_1^3} + \frac{A(x^2+z^2-2x_0x-2z_0z)k^2}{4\pi r_1^3}\Big]E_0\exp\{i(\omega t - kz_0(1+\frac{x_0^2+y_0^2}{2z_0^2}+\frac{r^2}{2z_0^2}-\frac{x_0x+y_0y+z_0z}{z_0^2}))\}\hat{\mathbf{y}}, \\
\Re\left\{\mathbf{E_{s_1}}\right\} &= -\Big[\frac{A(x_0^2+z_0^2)k^2}{4\pi r_1^3} + \frac{A(x^2+z^2-2x_0x-2z_0z)k^2}{4\pi r_1^3}\Big]E_0\cos\{(\omega t - kr_1)\}\hat{\mathbf{y}} \\
&\approx -\Big[\frac{A(x_0^2+z_0^2)k^2}{4\pi r_0^3} - \frac{A(x_0x+z_0z)k^2}{2\pi r_0^3}\Big]E_0\cos\{(\omega t - kr_1)\}\hat{\mathbf{y}} \\
&\approx -\Big[\frac{A(x_0^2+z_0^2)k^2}{4\pi r_0^3} - \frac{z_0zAk^2}{2\pi r_0^3} - \frac{x_0xAk^2}{2\pi r_0^3}\Big]E_0\cos\{(\omega t - kz_0(1+\frac{x_0^2+y_0^2}{2z_0^2}+\frac{r^2}{2z_0^2}-\frac{x_0x+y_0y+z_0z}{z_0^2}))\}\hat{\mathbf{y}}
\end{aligned} \tag{A3}$$

and

$$\begin{aligned}
\mathbf{E_{s_2}} &= \frac{Ak^2E_0}{4\pi r_2}\exp\{i(\omega t - kr_2)\}\Big[-\frac{(x_0+\Delta x+x)(y_0-y)}{r_2^2}\hat{\mathbf{x}} - \frac{(x_0+\Delta x+x)^2+(z_0-z)^2}{r_2^2}\hat{\mathbf{y}} + \frac{(z_0-z)(y_0-y)}{r_2^2}\hat{\mathbf{z}}\Big] \\
&\approx -\frac{Ak^2E_0}{4\pi r_2}\exp\{i(\omega t - kr_2)\}\Big[\frac{(x_0+\Delta x+x)^2+(z_0-z)^2}{r_2^2}\Big]\hat{\mathbf{y}} \\
&= -\Big[\frac{A(x_0^2+z_0^2)k^2}{4\pi r_2^3} + \frac{A(x^2+z^2+2x_0x-2z_0z)k^2}{4\pi r_2^3} + \frac{A(\Delta x^2+2x_0\Delta x+2x\Delta x)k^2}{4\pi r_2^3}\Big]E_0\exp\{i(\omega t - kr_2)\}\hat{\mathbf{y}} \\
&\approx -\Big[\frac{A(x_0^2+z_0^2)k^2}{4\pi r_2^3} + \frac{A(x^2+z^2+2x_0x-2z_0z)k^2}{4\pi r_2^3} + \frac{\Delta xx_0Ak^2}{2\pi r_0^3}\Big]E_0\exp\{i(\omega t - kr_2)\}\hat{\mathbf{y}} \\
&= -\Big[\frac{A(x_0^2+z_0^2)k^2}{4\pi r_2^3} + \frac{A(x^2+z^2-2z_0z)k^2}{4\pi r_2^3} + \frac{x_0xAk^2}{2\pi r_2^3} + \frac{\Delta xx_0Ak^2}{2\pi r_2^3}\Big]E_0 \\
&\quad\times\exp\{i(\omega t - kz_0(1+\frac{x_0^2+y_0^2}{2z_0^2}+\frac{r^2}{2z_0^2}+\frac{x_0x-y_0y-z_0z}{z_0^2}+\frac{\Delta xx_0}{z_0^2}))\}\hat{\mathbf{y}}, \\
\Re\left\{\mathbf{E_{s_2}}\right\} &= -\Big[\frac{A(x_0^2+z_0^2)k^2}{4\pi r_0^3} - \frac{z_0zAk^2}{2\pi r_2^3} + \frac{x_0xAk^2}{2\pi r_2^3} + \frac{\Delta xx_0Ak^2}{2\pi r_2^3}\Big]E_0\cos\{(\omega t - kz_0(1+\frac{x_0^2+y_0^2}{2z_0^2}+\frac{r^2}{2z_0^2}+\frac{x_0x-y_0y-z_0z}{z_0^2}+\frac{\Delta xx_0}{z_0^2}))\}\hat{\mathbf{y}},
\end{aligned} \tag{A4}$$

where $r_1 \approx z_0 + \frac{x_0^2+y_0^2}{2z_0} + \frac{r^2}{2z_0} - \frac{x_0x+y_0y+z_0z}{z_0}$ and $r_2 \approx z_0 + \frac{x_0^2+y_0^2}{2z_0} + \frac{r^2}{2z_0} + \frac{x_0x-y_0y-z_0z}{z_0} + \frac{\Delta xx_0}{z_0}$.

Considering the scattered field, and the field due to the directly transmitted light ($\mathbf{E_{T_1}}$ or $\mathbf{E_{T_2}}$) together, the overall field at the two photodiodes can be written as

$$\begin{aligned}
\mathbf{E_{D_1}} &\approx \frac{z_rE_0}{z_0}\exp\Big[i\omega t - ikz_0(1+\frac{x_0^2+y_0^2}{2z_0^2}) + \pi/2\Big] - \Big[\frac{A(x_0^2+z_0^2)k^2}{4\pi r_2^3} + \frac{A(x^2+z^2-2z_0z)k^2}{4\pi r_2^3} - \frac{x_0xAk^2}{2\pi r_2^3}\Big] \\
&\quad\times E_0\exp\{i(\omega t - kz_0(1+\frac{x_0^2+y_0^2}{2z_0^2}+\frac{r^2}{2z_0^2}-\frac{x_0x+y_0y+z_0z}{z_0^2}))\}\hat{\mathbf{y}}, \\
\mathbf{E_{D_2}} &\approx \frac{z_rE_0}{z_0}\exp\Big[i\omega t - ikz_0(1+\frac{x_0^2+y_0^2}{2z_0^2}) + \pi/2\Big]\exp(-i\frac{\Delta xx_0k}{z_0}) - \Big[\frac{A(x_0^2+z_0^2)k^2}{4\pi r_2^3} + \frac{A(x^2+z^2-2z_0z)k^2}{4\pi r_2^3} + \frac{x_0xAk^2}{2\pi r_2^3} + \frac{\Delta xx_0Ak^2}{2\pi r_2^3}\Big] \\
&\quad\times E_0\exp\{i(\omega t - kz_0(1+\frac{x_0^2+y_0^2}{2z_0^2}+\frac{r^2}{2z_0^2}+\frac{x_0x-y_0y-z_0z}{z_0^2}+\frac{\Delta xx_0}{z_0^2}))\}\hat{\mathbf{y}},
\end{aligned} \tag{A5}$$

where we have assumed $x_0, y_0, x, y, z << z_0$. Further, we have assumed that the depolarization of the scattered light is negligible. This is true when the levitated particle is small ($a << \lambda$) compared to the trapping laser's wavelength. The respective intensities

can be expressed as

$$
\begin{aligned}
I_{D_1} &= \frac{\epsilon_0 c E_{D_1} E_{D_1}^*}{2} \\
&= \frac{\epsilon_0 c z_r^2 E_0^2}{2z_0^2} + \Big[\frac{A(x_0^2+z_0^2)k^2}{4\pi z_0^3} + \frac{A(x^2+z^2-2z_0z)k^2}{4\pi z_0^3} - \frac{x_0 x A k^2}{2\pi z_0^3}\Big]^2 \frac{\epsilon_0 c E_0^2}{2} \\
&\quad - 2\frac{z_r \epsilon_0 c E_0^2}{2z_0}\Big[\frac{A(x_0^2+z_0^2)k^2}{4\pi z_0^3} + \frac{A(x^2+z^2-2z_0z)k^2}{4\pi z_0^3} - \frac{x_0 x A k^2}{2\pi z_0^3}\Big] \sin\Big(k\big(\frac{r^2}{2z_0} - \frac{x_0 x + y_0 y + z_0 z}{z_0}\big)\Big) \\
&\approx \frac{\epsilon_0 c z_r^2 E_0^2}{2z_0^2} + \Big[\frac{A(x_0^2+z_0^2)k^2}{4\pi z_0^3} + \frac{A(x^2+z^2-2z_0z)k^2}{4\pi z_0^3} - \frac{x_0 x A k^2}{2\pi z_0^3}\Big]^2 \frac{\epsilon_0 c E_0^2}{2} \\
&\quad - 2\frac{z_r \epsilon_0 c E_0^2}{2z_0}\Big[\frac{A(x_0^2+z_0^2)k^2}{4\pi z_0^3} + \frac{A(x^2+z^2-2z_0z)k^2}{4\pi z_0^3} - \frac{x_0 x A k^2}{2\pi z_0^3}\Big] \sin\Big(k\big(\frac{r^2-2y_0y-2z_0z}{2z_0} - \frac{x_0 x}{z_0}\big)\Big) \\
&= \frac{\epsilon_0 c z_r^2 E_0^2}{2z_0^2} + \Big[\frac{A(x_0^2+z_0^2)k^2}{4\pi z_0^3} + \frac{A(x^2+z^2-2z_0z)k^2}{4\pi z_0^3} - \frac{x_0 x A k^2}{2\pi z_0^3}\Big]^2 \frac{\epsilon_0 c E_0^2}{2} \\
&\quad - 2\Big[\frac{A(x_0^2+z_0^2)k^2}{4\pi z_0^3} + \frac{A(x^2+z^2-2z_0z)k^2}{4\pi z_0^3}\Big] \sin\Big(k\big(\frac{r^2-2y_0y-2z_0z}{2z_0} - \frac{x_0 x}{z_0}\big)\Big)\frac{z_r \epsilon_0 c E_0^2}{2z_0} \\
&\quad + 2\frac{x_0 x A k^2}{2\pi z_0^3} \sin\Big(k\big(\frac{r^2-2y_0y-2z_0z}{2z_0} - \frac{x_0 x}{z_0}\big)\Big)\frac{z_r \epsilon_0 c E_0^2}{2z_0}
\end{aligned} \tag{A6}
$$

and

$$
\begin{aligned}
I_{D_2} &= \frac{\epsilon_0 c E_{D_2} E_{D_2}^*}{2} \\
&= \frac{\epsilon_0 c z_r^2 E_0^2}{2z_0^2} + \Big(\frac{A(x_0^2+z_0^2)k^2}{4\pi z_0^3} + \frac{A(x^2+z^2-2z_0z)k^2}{4\pi z_0^3} + \frac{x_0 x A k^2}{2\pi z_0^3} + \frac{\Delta x x_0 A k^2}{2\pi z_0^3}\Big)^2 \frac{\epsilon_0 c E_0^2}{2} \\
&\quad - 2\Big(\frac{A(x_0^2+z_0^2)k^2}{4\pi z_0^3} + \frac{A(x^2+z^2-2z_0z)k^2}{4\pi z_0^3} + \frac{x_0 x A k^2}{2\pi z_0^3} + \frac{\Delta x x_0 A k^2}{2\pi z_0^3}\Big)\frac{z_r \epsilon_0 c E_0^2}{2z_0} \sin\Big(k\big(\frac{r^2}{2z_0} + \frac{x_0 x - y_0 y - z_0 z}{z_0} + \frac{\Delta x x_0}{z_0}\big)\Big) \\
&= \frac{\epsilon_0 c z_r^2 E_0^2}{2z_0^2} + \Big(\frac{A(x_0^2+z_0^2)k^2}{4\pi z_0^3} + \frac{A(x^2+z^2-2z_0z)k^2}{4\pi z_0^3} + \frac{x_0 x A k^2}{2\pi z_0^3} + \frac{\Delta x x_0 A k^2}{2\pi z_0^3}\Big)^2 \frac{\epsilon_0 c E_0^2}{2} \\
&\quad - 2\Big(\frac{A(x_0^2+z_0^2)k^2}{4\pi z_0^3} + \frac{A(x^2+z^2-2z_0z)k^2}{4\pi z_0^3} + \frac{x_0 x A k^2}{2\pi z_0^3} + \frac{\Delta x x_0 A k^2}{2\pi z_0^3}\Big)\frac{z_r \epsilon_0 c E_0^2}{2z_0} \sin\Big(k\big(\frac{r^2-2y_0y-2z_0z}{2z_0} + \frac{x_0 x}{z_0} + \frac{\Delta x x_0}{z_0}\big)\Big) \\
&= \frac{\epsilon_0 c z_r^2 E_0^2}{2z_0^2} + \Big(\frac{A(x_0^2+z_0^2)k^2}{4\pi z_0^3} + \frac{A(x^2+z^2-2z_0z)k^2}{4\pi z_0^3} + \frac{x_0 x A k^2}{2\pi z_0^3} + \frac{\Delta x x_0 A k^2}{2\pi z_0^3}\Big)^2 \frac{\epsilon_0 c E_0^2}{2} \\
&\quad - 2\Big(\frac{A(x_0^2+z_0^2)k^2}{4\pi z_0^3} + \frac{A(x^2+z^2-2z_0z)k^2}{4\pi z_0^3} + \frac{x_0 x A k^2}{2\pi z_0^3} + \frac{\Delta x x_0 A k^2}{2\pi z_0^3}\Big)\frac{z_r \epsilon_0 c E_0^2}{2z_0} \Big[\sin\Big(k\big(\frac{r^2-2y_0y-2z_0z}{2z_0} + \frac{x_0 x}{z_0}\big)\Big)\cos\big(\frac{\Delta x x_0 k}{z_0}\big) \\
&\quad + \cos\Big(k\big(\frac{r^2-2y_0y-2z_0z}{2z_0} + \frac{x_0 x}{z_0}\big)\Big)\sin\big(\frac{\Delta x x_0 k}{z_0}\big)\Big] \\
&\approx \frac{\epsilon_0 c z_r^2 E_0^2}{2z_0^2} + \Big(\frac{A(x_0^2+z_0^2)k^2}{4\pi z_0^3} + \frac{A(x^2+z^2-2z_0z)k^2}{4\pi z_0^3} + \frac{x_0 x A k^2}{2\pi z_0^3} + \frac{\Delta x x_0 A k^2}{2\pi z_0^3}\Big)^2 \frac{\epsilon_0 c E_0^2}{2} \\
&\quad - 2\Big(\frac{A(x_0^2+z_0^2)k^2}{4\pi z_0^3} + \frac{A(x^2+z^2-2z_0z)k^2}{4\pi z_0^3} + \frac{x_0 x A k^2}{2\pi z_0^3} + \frac{\Delta x x_0 A k^2}{2\pi z_0^3}\Big)\frac{z_r \epsilon_0 c E_0^2}{2z_0} \Big[\sin\Big(k\big(\frac{r^2-2y_0y-2z_0z}{2z_0} + \frac{x_0 x}{z_0}\big)\Big) \\
&\quad + \frac{\Delta x x_0 k}{z_0}\cos\Big(k\big(\frac{r^2-2y_0y-2z_0z}{2z_0} + \frac{x_0 x}{z_0}\big)\Big)\Big]
\end{aligned}
$$

$$
\begin{aligned}
&= \frac{\epsilon_0 c z_r^2 E_0^2}{2z_0^2} + \Big(\frac{A(x_0^2+z_0^2)k^2}{4\pi z_0^3} + \frac{A(x^2+z^2-2z_0z)k^2}{4\pi z_0^3} + \frac{x_0xAk^2}{2\pi z_0^3} + \frac{\Delta x x_0 Ak^2}{2\pi z_0^3}\Big)^2 \frac{\epsilon_0 c E_0^2}{2} \\
&- 2\Big(\frac{A(x_0^2+z_0^2)k^2}{4\pi z_0^3} + \frac{A(x^2+z^2-2z_0z)k^2}{4\pi z_0^3} + \frac{x_0xAk^2}{2\pi z_0^3} + \frac{\Delta x x_0 Ak^2}{2\pi z_0^3}\Big) \sin\Big(k\big(\frac{r^2-2y_0y-2z_0z}{2z_0} + \frac{x_0x}{z_0}\big)\Big) \frac{z_r\epsilon_0 c E_0^2}{2z_0} \\
&- \frac{2\Delta x x_0 k}{z_0}\Big(\frac{A(x_0^2+z_0^2)k^2}{4\pi z_0^3} + \frac{A(x^2+z^2-2z_0z)k^2}{4\pi z_0^3} + \frac{x_0xAk^2}{2\pi z_0^3} + \frac{\Delta x x_0 Ak^2}{2\pi z_0^3}\Big) \cos\Big(k\big(\frac{r^2-2y_0y-2z_0z}{2z_0} + \frac{x_0x}{z_0}\big)\Big) \frac{z_r\epsilon_0 c E_0^2}{2z_0} \\
&= \frac{\epsilon_0 c z_r^2 E_0^2}{2z_0^2} + \Big(\frac{A(x_0^2+z_0^2)k^2}{4\pi z_0^3} + \frac{A(x^2+z^2-2z_0z)k^2}{4\pi z_0^3} + \frac{x_0xAk^2}{2\pi z_0^3} + \frac{\Delta x x_0 Ak^2}{2\pi z_0^3}\Big)^2 \frac{\epsilon_0 c E_0^2}{2} \\
&- 2\Big(\frac{A(x_0^2+z_0^2)k^2}{4\pi z_0^3} + \frac{A(x^2+z^2-2z_0z)k^2}{4\pi z_0^3} + \frac{x_0xAk^2}{2\pi z_0^3}\Big) \sin\Big(k\big(\frac{r^2-2y_0y-2z_0z}{2z_0} + \frac{x_0x}{z_0}\big)\Big) \frac{z_r\epsilon_0 c E_0^2}{2z_0} \\
&- \frac{2\Delta x x_0 k}{z_0}\Big(\frac{A(x_0^2+z_0^2)k^2}{4\pi z_0^3} + \frac{A(x^2+z^2-2z_0z)k^2}{4\pi z_0^3} + \frac{x_0xAk^2}{2\pi z_0^3} + \frac{\Delta x x_0 Ak^2}{2\pi z_0^3}\Big) \cos\Big(k\big(\frac{r^2-2y_0y-2z_0z}{2z_0} + \frac{x_0x}{z_0}\big)\Big) \frac{z_r\epsilon_0 c E_0^2}{2z_0} \\
&= \frac{\epsilon_0 c z_r^2 E_0^2}{2z_0^2} + \Big(\frac{A(x_0^2+z_0^2)k^2}{4\pi z_0^3} + \frac{A(x^2+z^2-2z_0z)k^2}{4\pi z_0^3} + \frac{x_0xAk^2}{2\pi z_0^3} + \frac{\Delta x x_0 Ak^2}{2\pi z_0^3}\Big)^2 \frac{\epsilon_0 c E_0^2}{2} \\
&- 2\Big(\frac{A(x_0^2+z_0^2)k^2}{4\pi z_0^3} + \frac{A(x^2+z^2-2z_0z)k^2}{4\pi z_0^3}\Big) \sin\Big(k\big(\frac{r^2-2y_0y-2z_0z}{2z_0} + \frac{x_0x}{z_0}\big)\Big) \frac{z_r\epsilon_0 c E_0^2}{2z_0} \\
&- 2\frac{x_0xAk^2}{2\pi z_0^3} \sin\Big(k\big(\frac{r^2-2y_0y-2z_0z}{2z_0} + \frac{x_0x}{z_0}\big)\Big) \frac{z_r\epsilon_0 c E_0^2}{2z_0} \\
&- \frac{2\Delta x x_0 k}{z_0}\Big(\frac{A(x_0^2+z_0^2)k^2}{4\pi z_0^3} + \frac{A(x^2+z^2-2z_0z)k^2}{4\pi z_0^3} + \frac{x_0xAk^2}{2\pi z_0^3} + \frac{\Delta x x_0 Ak^2}{2\pi z_0^3}\Big) \cos\Big(k\big(\frac{r^2-2y_0y-2z_0z}{2z_0} + \frac{x_0x}{z_0}\big)\Big) \frac{z_r\epsilon_0 c E_0^2}{2z_0}. \qquad \text{(A7)}
\end{aligned}
$$

$$
\begin{aligned}
\Delta I &= I_{D_2} - I_{D_1} \\
&= \frac{\epsilon_0 c E_{D_2} E_{D_2}^*}{2} - \frac{\epsilon_0 c E_{D_1} E_{D_1}^*}{2}. \qquad \text{(A8)}
\end{aligned}
$$

The difference between I_{D_2} and I_{D_1} is

$$
\begin{aligned}
\Delta I &= \Big[\frac{A(x_0^2+z_0^2)k^2}{4\pi z_0^3} + \frac{A(x^2+z^2-2z_0z)k^2}{4\pi z_0^3} + \frac{x_0xAk^2}{2\pi z_0^3} + \frac{\Delta x x_0 Ak^2}{2\pi z_0^3}\Big]^2 \frac{\epsilon_0 c E_0^2}{2} \\
&- \Big[\frac{A(x_0^2+z_0^2)k^2}{4\pi z_0^3} + \frac{A(x^2+z^2-2z_0z)k^2}{4\pi z_0^3} - \frac{x_0xAk^2}{2\pi z_0^3}\Big]^2 \frac{\epsilon_0 c E_0^2}{2} \\
&- 2\Big[\frac{A(x_0^2+z_0^2)k^2}{4\pi z_0^3} + \frac{A(x^2+z^2-2z_0z)k^2}{4\pi z_0^3}\Big] \sin\Big(k\big(\frac{r^2-2y_0y-2z_0z}{2z_0} + \frac{x_0x}{z_0}\big)\Big) \frac{z_r\epsilon_0 c E_0^2}{2z_0} \\
&+ 2\Big[\frac{A(x_0^2+z_0^2)k^2}{4\pi z_0^3} + \frac{A(x^2+z^2-2z_0z)k^2}{4\pi z_0^3}\Big] \sin\Big(k\big(\frac{r^2-2y_0y-2z_0z}{2z_0} - \frac{x_0x}{z_0}\big)\Big) \frac{z_r\epsilon_0 c E_0^2}{2z_0} \\
&- 2\frac{x_0xAk^2}{2\pi z_0^3} \sin\Big(k\big(\frac{r^2-2y_0y-2z_0z}{2z_0} + \frac{x_0x}{z_0}\big)\Big) \frac{z_r\epsilon_0 c E_0^2}{2z_0} \\
&- 2\frac{x_0xAk^2}{2\pi z_0^3} \sin\Big(k\big(\frac{r^2-2y_0y-2z_0z}{2z_0} - \frac{x_0x}{z_0}\big)\Big) \frac{z_r\epsilon_0 c E_0^2}{2z_0} \\
&- \frac{2\Delta x x_0 k}{z_0}\Big(\frac{A(x_0^2+z_0^2)k^2}{4\pi z_0^3} + \frac{A(x^2+z^2-2z_0z)k^2}{4\pi z_0^3} + \frac{x_0xAk^2}{2\pi z_0^3} + \frac{\Delta x x_0 Ak^2}{2\pi z_0^3}\Big) \cos\Big(k\big(\frac{r^2-2y_0y-2z_0z}{2z_0} + \frac{x_0x}{z_0}\big)\Big) \frac{z_r\epsilon_0 c E_0^2}{2z_0}
\end{aligned}
$$

$$
\begin{aligned}
&= \Big[\frac{A(x_0^2+z_0^2)k^2}{4\pi z_0^3} + \frac{A(x^2+z^2-2z_0z)k^2}{4\pi z_0^3} + \frac{x_0xAk^2}{2\pi z_0^3} + \frac{\Delta x x_0 Ak^2}{2\pi z_0^3}\Big]^2 \frac{\epsilon_0 cE_0^2}{2} \\
&\quad - \Big[\frac{A(x_0^2+z_0^2)k^2}{4\pi z_0^3} + \frac{A(x^2+z^2-2z_0z)k^2}{4\pi z_0^3} - \frac{x_0xAk^2}{2\pi z_0^3}\Big]^2 \frac{\epsilon_0 cE_0^2}{2} \\
&\quad - 4\Big(\frac{A(x_0^2+z_0^2)k^2}{4\pi z_0^3} + \frac{A(x^2+z^2-2z_0z)k^2}{4\pi z_0^3}\Big)\cos\Big(k\frac{r^2-2y_0y-2z_0z}{2z_0}\Big)\sin\Big(\frac{x_0xk}{z_0}\Big)\frac{z_r\epsilon_0 cE_0^2}{2z_0} \\
&\quad - 4\frac{x_0xAk^2}{2\pi z_0^3}\sin\Big(k\frac{r^2-2y_0y-2z_0z}{2z_0}\Big)\cos\Big(\frac{x_0xk}{z_0}\Big)\frac{z_r\epsilon_0 cE_0^2}{2z_0} \\
&\quad - \frac{2\Delta x x_0 k}{z_0}\Big(\frac{A(x_0^2+z_0^2)k^2}{4\pi z_0^3} + \frac{A(x^2+z^2-2z_0z)k^2}{4\pi z_0^3} + \frac{x_0xAk^2}{2\pi z_0^3} + \frac{\Delta x x_0 Ak^2}{2\pi z_0^3}\Big)\cos\Big(k(\frac{r^2-2y_0y-2z_0z}{2z_0} + \frac{x_0x}{z_0})\Big)\frac{z_r\epsilon_0 cE_0^2}{2z_0} \\
&\approx \overbrace{\frac{x_0xA^2k^4}{2\pi^2 z_0^6}\Big(x_0^2+z_0^2+x^2+z^2-2z_0z\Big)I_0}^{Scattering} - \overbrace{\frac{Ak^2}{\pi z_0^3}\Big(x_0^2+z_0^2+x^2+z^2-2z_0z\Big)\cos\Big(k\frac{r^2-2y_0y-2z_0z}{2z_0}\Big)\sin\Big(\frac{x_0xk}{z_0}\Big)\frac{z_r}{z_0}I_0}^{Interference} \\
&\quad \overbrace{- 4\frac{x_0xAk^2}{2\pi z_0^3}\sin\Big(k\frac{r^2-2y_0y-2z_0z}{2z_0}\Big)\cos\Big(\frac{x_0xk}{z_0}\Big)\frac{z_r\epsilon_0 cE_0^2}{2z_0}}^{Interference} \\
&\quad \overbrace{- \frac{\Delta x x_0 Ak^3}{2\pi z_0^4}\Big(x_0^2+z_0^2+x^2+z^2-2z_0z+2x_0x\Big)\cos\Big(k(\frac{r^2-2y_0y-2z_0z}{2z_0}+\frac{x_0x}{z_0})\Big)\frac{z_r}{z_0}I_0}^{Imbalance} \overbrace{\frac{\Delta x x_0 A^2k^4}{4\pi^2 z_0^6}\Big(x_0^2+z_0^2+x^2+z^2-2z_0z\Big)I_0}^{Imbalance} \\
&= \overbrace{\frac{x_0xA^2k^4}{2\pi^2 z_0^6}\Big(x_0^2+z_0^2+x^2+z^2-2z_0z\Big)I_0}^{Scattering} - \overbrace{\frac{z_rAk^2}{\pi z_0^4}\Big(x_0^2+z_0^2+x^2+z^2-2z_0z\Big)\Big(1-\frac{k^2(r^2-2y_0y-2z_0z)^2}{8z_0^2}\Big)\frac{x_0xk}{z_0}I_0}^{Interference} \\
&\quad \overbrace{- 4\frac{x_0xAk^2}{2\pi z_0^3}\Big(k\frac{r^2-2y_0y-2z_0z}{2z_0} - k^3\frac{(r^2-2y_0y-2z_0z)^3}{48z_0^3}\Big)\Big(1-\frac{x_0^2x^2k^2}{2z_0^2}\Big)\frac{z_r\epsilon_0 cE_0^2}{2z_0}}^{Interference} \\
&\quad \overbrace{- \frac{\Delta x x_0 Ak^3}{2\pi z_0^4}\Big(x_0^2+z_0^2+x^2+z^2-2z_0z+2x_0x\Big)\cos\Big(k(\frac{r^2-2y_0y-2z_0z}{2z_0}+\frac{x_0x}{z_0})\Big)\frac{z_r}{z_0}I_0}^{Imbalance} + \overbrace{\frac{\Delta x x_0 A^2k^4}{4\pi^2 z_0^6}\Big(x_0^2+z_0^2+x^2+z^2-2z_0z\Big)I_0}^{Imbalance} \\
&\approx \overbrace{\frac{x_0xA^2k^4}{2\pi^2 z_0^6}\Big(x_0^2+z_0^2+x^2+z^2-2z_0z\Big)I_0}^{Scattering} - \overbrace{\frac{x_0z_rAk^3}{\pi z_0^5}x\Big(x_0^2+z_0^2+x^2+z^2-2z_0z\Big)\Big(1-\frac{k^2(r^2-2y_0y-2z_0z)^2}{8z_0^2}\Big)I_0}^{Interference} \\
&\quad \overbrace{- 4\frac{x_0xAk^2}{2\pi z_0^3}\Big(k\frac{r^2-2y_0y-2z_0z}{2z_0} - k^3\frac{(r^2-2y_0y-2z_0z)^3}{48z_0^3}\Big)\Big(1-\frac{x_0^2x^2k^2}{2z_0^2}\Big)\frac{z_r\epsilon_0 cE_0^2}{2z_0}}^{Interference} \\
&\quad \overbrace{- \frac{\Delta x x_0 z_rAk^3}{2\pi z_0^5}\Big(x_0^2+z_0^2+x^2+z^2-2z_0z+2x_0x\Big)\cos\Big(k(\frac{r^2-2y_0y-2z_0z}{2z_0}+\frac{x_0x}{z_0})\Big)I_0}^{Imbalance}, \qquad \text{(A9)}
\end{aligned}
$$

where $I_0 = \epsilon_0 cE_0^2/2$. In order to compare the validity of Eq. (A9), Fig. 5 shows a comparison between Eqs. (A8) and (A9) where various approximations have been made. It can be seen that they match quite well.

From Eq. (A9), the interference term is

$$
\begin{aligned}
\Delta I_{Inter} \approx &-\frac{x_0z_rAk^3}{\pi z_0^5}x\Big(x_0^2+z_0^2+x^2+z^2-2z_0z\Big)\Big(1-\frac{k^2(r^2-2y_0y-2z_0z)^2}{8z_0^2}\Big)I_0 \\
&-2\frac{x_0z_rxAk^2}{\pi z_0^4}\Big(k\frac{r^2-2y_0y-2z_0z}{2z_0} - k^3\frac{(r^2-2y_0y-2z_0z)^3}{48z_0^3}\Big)\Big(1-\frac{x_0^2x^2k^2}{2z_0^2}\Big)I_0
\end{aligned}
$$

$$
\begin{aligned}
&\approx -\frac{x_0 z_r A k^3}{\pi z_0^5} x\Big[x_0^2+z_0^2+x^2+z^2-2z_0z-\frac{k^2(x_0^2+z_0^2+x^2+z^2-2z_0z)(r^2-2y_0y-2z_0z)^2}{8z_0^2}\Big]I_0\\
&\quad -2\frac{x_0 z_r x A k^2}{\pi z_0^4}\Big(k\frac{r^2-2y_0y-2z_0z}{2z_0}-k^3\frac{(r^2-2y_0y-2z_0z)^3}{48z_0^3}\Big)I_0\\
&\approx -\frac{x_0 z_r A k^3}{\pi z_0^5} x\Big[x_0^2+z_0^2+x^2+z^2-2z_0z-\frac{k^2(x_0^2+z_0^2)(r^2-2y_0y-2z_0z)^2}{8z_0^2}\Big]I_0-\frac{x_0 z_r A k^3}{\pi z_0^5}x(r^2-2y_0y-2z_0z)I_0\\
&= -\frac{x_0 z_r A k^3}{\pi z_0^5}\Big[(x_0^2+z_0^2)x+x^3+xz^2-2z_0xz+x(r^2-2y_0y-2z_0z)+\frac{xk^2(x_0^2+z_0^2)(r^2-2y_0y-2z_0z)^2}{8z_0^2}\Big]I_0\\
&= -\frac{x_0 z_r A k^3}{\pi z_0^5}\Big[(x_0^2+z_0^2)x+x^3+xz^2-2z_0xz+x^3+xy^2+xz^2-2y_0xy-2z_0xz-\frac{xk^2(x_0^2+z_0^2)(r^2-2y_0y-2z_0z)^2}{8z_0^2}\Big]I_0\\
&= -\frac{x_0 z_r A k^3}{\pi z_0^5}\Big[(x_0^2+z_0^2)x-4z_0xz-2y_0xy+2x^3+xy^2+2xz^2-\frac{xk^2(x_0^2+z_0^2)(r^2-2y_0y-2z_0z)^2}{8z_0^2}\Big]I_0\\
&= -\frac{x_0 z_r A k^3}{\pi z_0^5}\Big[(x_0^2+z_0^2)A_x\sin\omega_x t-4z_0A_xA_z\sin\omega_x t\sin\omega_z t-2y_0A_xA_y\sin\omega_x t\sin\omega_y t+2x^3+xy^2+2xz^2\\
&\quad -\frac{xk^2(x_0^2+z_0^2)(r^2-2y_0y-2z_0z)^2}{8z_0^2}\Big]I_0\\
&= -\frac{x_0 z_r A k^3}{\pi z_0^5}\Big[(x_0^2+z_0^2)A_x\sin\omega_x t-4z_0A_xA_z\sin\omega_x t\sin\omega_z t-2y_0xy+2x^3+xy^2+2xz^2\\
&\quad -\frac{xk^2(x_0^2+z_0^2)(r^2-2y_0y-2z_0z)^2}{8z_0^2}\Big]I_0\\
&= -\frac{x_0 z_r A k^3}{\pi z_0^5}\Big[(x_0^2+z_0^2)A_x\sin\omega_x t-2z_0A_xA_z\cos(\omega_x-\omega_z)t+2z_0A_xA_z\cos(\omega_x+\omega_z)t-2y_0xy\\
&\quad +2x^3+xy^2+2xz^2-\frac{xk^2(x_0^2+z_0^2)(r^2-2y_0y-2z_0z)^2}{8z_0^2}\Big]I_0\\
&= -\frac{x_0 z_r A k^3}{\pi z_0^5}\Big[(x_0^2+z_0^2)A_x\sin\omega_x t-2z_0A_xA_z\cos(\omega_x-\omega_z)t+2z_0A_xA_z\cos(\omega_x+\omega_z)t+\mathrm{f}(\omega_\mathrm{x},\omega_\mathrm{y},\omega_z)\Big]I_0. \qquad \text{(A10)}
\end{aligned}
$$

Likewise the term due to the imbalance can be written as

$$
\begin{aligned}
\Delta I_{Imb} &= -\frac{\alpha z_r A k^2}{2\pi z_0^4}\Big(x_0^2+z_0^2+x^2+z^2-2z_0z+2x_0x\Big)\cos\Big(k(\frac{r^2-2y_0y-2z_0z}{2z_0}+\frac{x_0x}{z_0})\Big)I_0+\frac{\alpha A^2k^3}{4\pi^2 z_0^5}\Big(x_0^2+z_0^2+x^2+z^2-2z_0z\Big)I_0\\
&\approx -\frac{\alpha z_r A k^2}{2\pi z_0^4}\Big(x_0^2+z_0^2+x^2+z^2-2z_0z+2x_0x\Big)\Big(1-\frac{k^2(r^2-2y_0y-2z_0z+2x_0x)^2}{8z_0^2}\Big)I_0\\
&= -\frac{\alpha z_r A k^2}{2\pi z_0^4}\Big[x_0^2+z_0^2+x^2+z^2-2z_0z+2x_0x-\frac{k^2(x_0^2+z_0^2+x^2+z^2-2z_0z+2x_0x)(r^2-2y_0y-2z_0z+2x_0x)^2}{8z_0^2}\Big]I_0\\
&= -\frac{\alpha z_r A k^2}{2\pi z_0^4}\Big[x_0^2+z_0^2-2z_0z+2x_0x+x^2+z^2-\frac{k^2(x_0^2+z_0^2+x^2+z^2-2z_0z+2x_0x)(r^2-2y_0y-2z_0z+2x_0x)^2}{8z_0^2}\Big]I_0. \qquad \text{(A11)}
\end{aligned}
$$

Finally, the signal that a balanced detector along the z-axis, excluding the DC component (see main text for details), produces can be expressed as

$$
\begin{aligned}
\Delta I_z &= \frac{\epsilon_0 c E_{D_1}E_{D_1}^*}{2}\\
&= \frac{\epsilon_0 c z_r^2 E_0^2}{2z_0^2}+\Big[\frac{A(x_0^2+z_0^2)k^2}{4\pi z_0^3}+\frac{A(x^2+z^2-2z_0z)k^2}{4\pi z_0^3}-\frac{x_0xAk^2}{2\pi z_0^3}\Big]^2\frac{\epsilon_0 c E_0^2}{2}\\
&\quad +2\frac{z_r\epsilon_0 c E_0^2}{2z_0}\Big[\frac{A(x_0^2+z_0^2)k^2}{4\pi z_0^3}+\frac{A(x^2+z^2-2z_0z)k^2}{4\pi z_0^3}-\frac{x_0xAk^2}{2\pi z_0^3}\Big]\sin\Big(k(\frac{r^2}{2z_0}-\frac{x_0x+y_0y+z_0z}{z_0})\Big)
\end{aligned}
$$

$$
\begin{aligned}
&\approx \frac{\epsilon_0 c z_r^2 E_0^2}{2z_0^2} + \Big[\frac{A(x_0^2+z_0^2)k^2}{4\pi z_0^3} + \frac{A(x^2+z^2-2z_0z)k^2}{4\pi z_0^3} - \frac{x_0xAk^2}{2\pi z_0^3}\Big]^2 \frac{\epsilon_0 c E_0^2}{2} \\
&\quad + 2\frac{z_r\epsilon_0 c E_0^2}{2z_0}\Big[\frac{A(x_0^2+z_0^2)k^2}{4\pi z_0^3} + \frac{A(x^2+z^2-2z_0z)k^2}{4\pi z_0^3} - \frac{x_0xAk^2}{2\pi z_0^3}\Big]\sin\Big(k(\frac{r^2-2y_0y-2z_0z}{2z_0} - \frac{x_0x}{z_0})\Big) \\
&= \frac{\epsilon_0 c z_r^2 E_0^2}{2z_0^2} + \Big[\frac{A(x_0^2+z_0^2)k^2}{4\pi z_0^3} + \frac{A(x^2+z^2-2z_0z)k^2}{4\pi z_0^3} - \frac{x_0xAk^2}{2\pi z_0^3}\Big]^2 \frac{\epsilon_0 c E_0^2}{2} \\
&\quad + 2\Big[\frac{A(x_0^2+z_0^2)k^2}{4\pi z_0^3} + \frac{A(x^2+z^2-2z_0z)k^2}{4\pi z_0^3}\Big]\sin\Big(k(\frac{r^2-2y_0y-2z_0z}{2z_0} - \frac{x_0x}{z_0})\Big)\frac{z_r\epsilon_0 c E_0^2}{2z_0} \\
&\quad - 2\frac{x_0xAk^2}{2\pi z_0^3}\sin\Big(k(\frac{r^2-2y_0y-2z_0z}{2z_0} - \frac{x_0x}{z_0})\Big)\frac{z_r\epsilon_0 c E_0^2}{2z_0} \\
&\approx \Big[\frac{A(x_0^2+z_0^2)k^2}{2\pi z_0^3} + \frac{A(x^2+z^2-2z_0z)k^2}{2\pi z_0^3}\Big]\sin\Big(\frac{k(r^2-2y_0y-2z_0z-2x_0x)}{2z_0}\Big)\frac{z_r}{z_0}I_0 \\
&\approx \Big[\frac{(x_0^2+z_0^2)(r^2-2y_0y-2z_0z-2x_0x)k^3A}{4\pi z_0^4} + \frac{(x^2+z^2-2z_0z)(r^2-2y_0y-2z_0z-2x_0x)k^3A}{4\pi z_0^4}\Big]\frac{z_r}{z_0}I_0 \\
&\approx \frac{(x_0^2+z_0^2)(r^2-2y_0y-2z_0z-2x_0x)z_rk^3A}{4\pi z_0^5}I_0 \\
&= \frac{z_r(x_0^2+z_0^2)k^3A}{4\pi z_0^5}(A_x^2\sin^2\omega_xt + A_y^2\sin^2\omega_yt + A_z^2\sin^2\omega_zt - 2x_0A_x\sin\omega_xt - 2y_0A_y\sin\omega_yt - 2z_0A_z\sin\omega_zt)I_0. \qquad \text{(A12)}
\end{aligned}
$$

[1] J. Gieseler, L. Novotny, and R. Quidant, Nat. Phys. **9**, 806 (2013).
[2] G. Ranjit, D. P. Atherton, J. H. Stutz, M. Cunningham, and A. A. Geraci, Phys. Rev. A **91**, 051805 (2015).
[3] G. Ranjit, M. Cunningham, K. Casey, and A. A. Geraci, Phys. Rev. A **93**, 053801 (2016).
[4] T. Li, S. Kheifets, and M. G. Raizen, Nat. Phys. **7**, 527 (2011).
[5] J. Gieseler, B. Deutsch, R. Quidant, and L. Novotny, Phys. Rev. Lett. **109**, 103603 (2012).
[6] V. Jain, J. Gieseler, C. Moritz, C. Dellago, R. Quidant, and L. Novotny, Phys. Rev. Lett. **116**, 243601 (2016).
[7] T. Li, S. Kheifets, D. Medellin, and M. G. Raizen, Science **328**, 1673 (2010).
[8] J. Gieseler, R. Quidant, C. Dellago, and L. Novotny, Nat. Nanotechnol. **9**, 358 (2014).
[9] J. Gieseler, M. Spasenović, L. Novotny, and R. Quidant, Phys. Rev. Lett. **112**, 103603 (2014).
[10] L. P. Neukirch, E. von Haartman, J. M. Rosenholm, and A. N. Vamivakas, Nat. Photonics **9**, 653–657 (2015).
[11] A. T. M. A. Rahman, A. C. Frangeskou, M. S. Kim, S. Bose, G. W. Morley, and P. F. Barker, Sci. Rep. **6**, 21633 (2016).
[12] J. Vovrosh, M. Rashid, D. Hempston, J. Bateman, M. Paternostro, and H. Ulbricht, J. Opt. Soc. Am. B **34**, 1421 (2017).
[13] C. Wan, M. Scala, S. Bose, A. C. Frangeskou, A. T. M. A. Rahman, G. W. Morley, P. F. Barker, and M. S. Kim, Phys. Rev. A **93**, 043852 (2016).
[14] A. T. M. A. Rahman and P. F. Barker, Nat. Photonics **11**, 634 (2017).
[15] B. E. A. Saleh and M. C. Teich, *Fundamentals of Photonics*, 2nd ed. (John Wiley, Hoboken, N.J., 2007).
[16] L. Novotny and B. Hecht, *Principles of Nano-Optics*, 2nd ed. (Cambridge University Press, 2012).
[17] R. P. Feynman, R. B. Leighton, and M. Sands, *The Feynman Lectures on Physics* (Addison-Wesley, 2005), Vol. I, Chap. 30.
[18] C. F. Bohren and D. R. Huffman, "Particles small compared with the wavelength," in *Absorption and Scattering of Light by Small Particles* (Wiley-VCH Verlag GmbH, 2007), pp. 130–157.